Multicolor Tuning

DOI: 10.1002/anie.200704520

Multicolor Tuning of (Ln, P)-Doped YVO_4 Nanoparticles by Single-Wavelength Excitation**

*Feng Wang, Xuejia Xue, and Xiaogang Liu**

Fluorescent probes enable researchers to encode chemical information and to detect particular components of complex biomolecular assemblies, such as live cells, with substantial sensitivity and selectivity.[1] Multicolor labeling experiments entail the deliberate introduction of two or more fluorescent probes to simultaneously monitor different biochemical functions. This approach has applications in areas as diverse as drug discovery, catalyst screening, DNA sequencing, fluorescent microscopy, and clinical diagnostics.[2] Ideal probes for multicolor labeling would exhibit considerable photochemical stability, strong absorption at a given excitation wavelength, and well-resolved emission spectra with narrow bandwidths. Most common dye probes have low photobleaching thresholds, require different excitation wavelengths, and exhibit broad emission spectra.[3] In contrast, quantum dots (QDs) exhibit relatively narrow emission band widths of 20 to 30 nm (full width at half maximum (FWHM)) under single-wavelength excitation,[4] but they can suffer from cytotoxicity in vivo, fluorescence intermittency, and limited distinguishable features in the emission spectra. Moreove, particles with a narrow size distribution (ca. 5%) often require stringent synthesis conditions.[5] The single emission peaks resulting from excitation of QDs of similar sizes make spectral interpretation difficult when overlapping spectral features become predominant.[5e]

As an alternative to dye molecules and QDs, lanthanide-doped nanoparticles have been suggested as a promising new class of fluorescent probes.[6] They show superior chemical and optical properties, including low toxicity, large effective Stokes shifts, sharp emission band widths of 10 to 20 nm (FWHM), as well as high resistance to photobleaching, blinking, and photochemical degradation.[6] More importantly, in contrast to single emission peaks observed for QDs, the Ln-doped nanoparticles generally show a distinct set of sharp emission peaks arising from f–f orbital electronic transitions. The multiple-peak patterns should provide spectroscopic fingerprints, which are particularly useful for accurate interpretation in the event of overlapping emission spectra. These unique properties, coupled with size- and shape-independent luminescent phenomena,[6a,c] make Ln-doped nanoparticles highly suitable fluorescent probes for multicolor labeling applications. Herein, we present two complementary approaches (tuning emission wavelength and relative intensity) to emission color modulation by single-wavelength excitation based upon (Ln, P)-doped YVO_4 host-lattice sensitized nanoparticle systems.

The YVO_4 nanoparticles doped with Ln and phosphorous ions were synthesized in aqueous media in the presence of polyvinylpyrrolidone (PVP). The metal-chelating PVP molecules stabilize the Ln ions and control the growth of nanoparticles upon reaction with $[VO_4]^{3-}$ and $[PO_4]^{3-}$ groups. Figure 1a,c shows typical transmission electron microscopy (TEM) images of the as-synthesized spherical

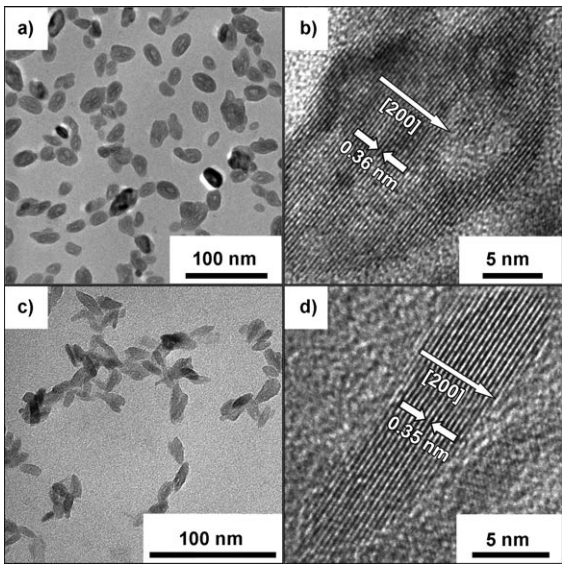

Figure 1. Typical TEM characterization of the (Ln, P)-doped nanoparticles. a) Low-resolution TEM image showing spherical $(Y_{0.95}Eu_{0.05})VO_4$ nanoparticles. b) High-resolution TEM image showing well-defined (200) lattice fringes of $(Y_{0.95}Eu_{0.05})VO_4$ nanoparticles with a *d* spacing of 0.36 nm. c,d) Low- and high-resolution TEM images, respectively, of rod-like $Y(P_{0.75}V_{0.25})O_4$ nanoparticles showing (200) lattice fringes with a *d* spacing of 0.35 nm.

$(Y_{0.95}Eu_{0.05})VO_4$ and rod-like $Y(P_{0.75}V_{0.25})O_4$ naonoparticles with average diameters of 20 and 10 nm, respectively. High-resolution TEM images shown in Figure 1b,d reveal the single-crystalline nature of the particles and lattice fringes with observed *d* spacings of 0.36 and 0.35 nm, which are in good agreement with the lattice spacing in the (200) planes of tetragonal YVO_4 (0.356 nm, Joint Committee on Powder Diffraction Standards file number 17-0341). Furthermore, the

[*] Dr. F. Wang, X. Xue, Prof. X. Liu
Department of Chemistry, National University of Singapore
3 Science Drive 3, Singapore 117543 (Singapore)
Fax: (+65) 6779-1691
E-mail: chmlx@nus.edu.sg

[**] This study was supported by a Start-Up Grant Award (Grant No. R-143-000-317) and a Young Investigator Award (Grant No. R-143-000-318) to X.L. by NUS. The authors thank C. N. Tang for taking HRTEM images.

high-resolution TEM image of Eu-doped nanoparticles (Figure 1b) shows the presence of hollow structures inside the particle. The as-synthesized nanoparticles are readily dispersed in aqueous and organic solvents (Figure 2). X-ray powder diffraction (XRD) patterns of the $(Y_{0.95}Eu_{0.05})VO_4$ and $Y(P_{0.75}V_{0.25})O_4$ naonoparticles are shown in Figure 3. Both samples exhibit diffraction patterns that can be easily indexed in accord with tetragonal xenotime YVO_4 crystals, suggesting high crystallinity of the products. The narrower XRD peaks for $(Y_{0.95}Eu_{0.05})VO_4$ than $Y(P_{0.75}V_{0.25})O_4$ indicate a larger average particle size for the former, which is consistent with the TEM analysis of the nanoparticles. It should also be noted that $Y(P_{0.75}V_{0.25})O_4$ nanoparticles exhibit a spectral shift toward higher diffraction angles, in contrast with the literature data. The spectral shift can be attributed to a large amount of ion substitution of V ions by the smaller P centers in the YVO_4 crystal lattice, resulting in a smaller unit-cell volume.[7]

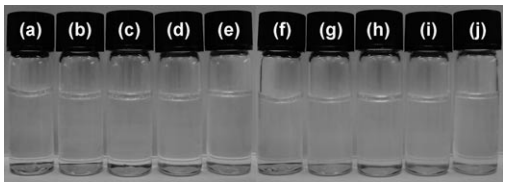

Figure 2. Photographs showing colloidal solutions (1 mM each) of a–e) $(Y_{0.95}Eu_{0.05})VO_4$ and f–j) $Y(P_{0.75}V_{0.25})O_4$ nanoparticles in water (a, f), ethanol (b, g), dimethylformamide (c, h), tetrahydrofuran (d, i), and dichloromethane (e, j).

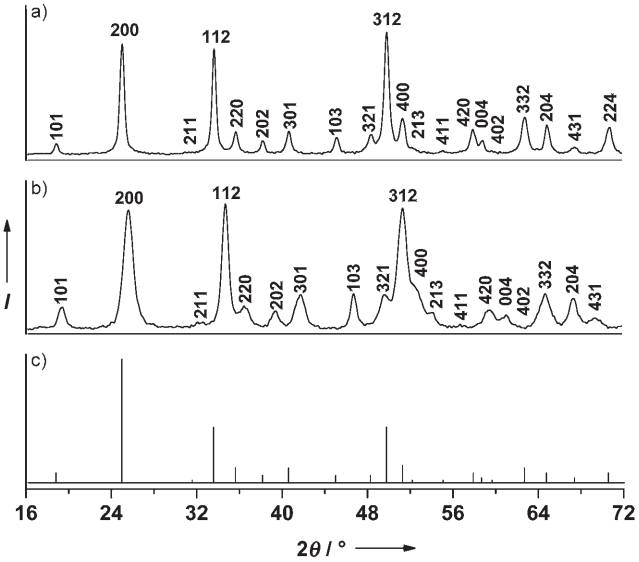

Figure 3. XRD patterns of the a) $(Y_{0.95}Eu_{0.05})VO_4$ and b) $Y(P_{0.75}V_{0.25})O_4$ nanoparticles. c) Literature data for xenotime YVO_4 crystals (Joint Committee on Powder Diffraction Standards file number 17-0341).

Photoluminescence studies were first carried out on Ln-doped YVO_4 nanoparticles. Under ultraviolet (UV) excitation on unactivated YVO_4, the excitation energy will readily migrate through $[VO_4]^{3-}$ groups to a quenching site (e.g. an impurity randomly located in the crystal lattice) and dissipate nonradiatively (Scheme 1a).[8] Owing to the strong coupling between the electrons and the vibrations of the $[VO_4]^{3-}$ center and relatively small (ca. 10000 cm^{-1}) Stokes shift in the $[VO_4]^{3-}$ emission, the thermally activated energy migration is so efficient that the host YVO_4 essentially does not show any visible emission at room temperature.[8] When selected lanthanide ions are incorporated into the YVO_4 nanoparticles, they function as activators and introduce characteristic emission through efficient energy transfer from the $[VO_4]^{3-}$ groups to the dopants. Thus, $[VO_4]^{3-}$ serves as a universal sensitizer for a wide range of lanthanide activators. As a proof-of-concept experiment, excitation and emission spectra for YVO_4 nanoparticles doped with Eu^{3+}, Dy^{3+}, and Sm^{3+} were acquired at room temperature in aqueous solutions (Figure 4). The excitation spectra were recorded by monitoring the emission of Eu^{3+}, Dy^{3+}, and Sm^{3+} at 618, 576, and 604 nm, respectively. The absorption spectra are nearly identical and exhibit an intense broad band centered at approximately 280 nm, which can be attributed to charge transfer within the $[VO_4]^{3-}$ groups. In the emission spectra, which were recorded with 280-nm excitation, characteristic sharp emission patterns can be observed and assigned to $^5D_{1,0}\rightarrow{}^7F_{0,1,2,3,4}$, $^4F_{9/2}\rightarrow{}^6H_{15/2,13/2,11/2}$, and $^4G_{5/2}\rightarrow{}^6H_{5/2,7/2,9/2,11/2}$ transitions for Eu^{3+}, Dy^{3+}, and Sm^{3+}, respectively. Corresponding visible emissions of the particle solutions (1 mM) upon excitation at 254 nm with a 4-W hand-held UV lamp are shown in Figure 4 (insets). Importantly, the photoluminescence intensity of these nanoparticles after UV irradiation for 24 h remains essentially unaltered, thus indicating high photostability of the nanoparticles.

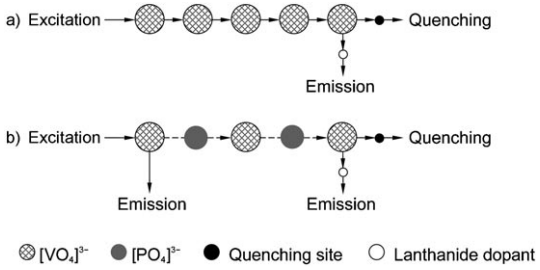

Scheme 1. Proposed energy-transfer mechanisms in a) Ln-doped and b) (Ln, P)-doped YVO_4 crystals. In Ln-doped YVO_4 crystals, energy transfer from $[VO_4]^{3-}$ to Ln^{3+} is highly efficient. In contrast, the energy transfer in (Ln, P)-doped YVO_4 crystals is less efficient owing to the increased V···V separation that results from phosphorus doping.

To demonstrate the versatility of the lanthanide-doping approach for multicolor emission, we also studied (Ln, P)-doped YVO_4 nanoparticles. We reasoned that introduction of phosphorus into the YVO_4 lattice would increase the V···V separation and thus hamper the efficient energy transfer from $[VO_4]^{3-}$ groups to the quenching sites. Consequently, the particles should show intense emission from the $[VO_4]^{3-}$ groups. Upon further addition of Ln dopants into the P-doped YVO_4 nanoparticles, a dual emission from the host and

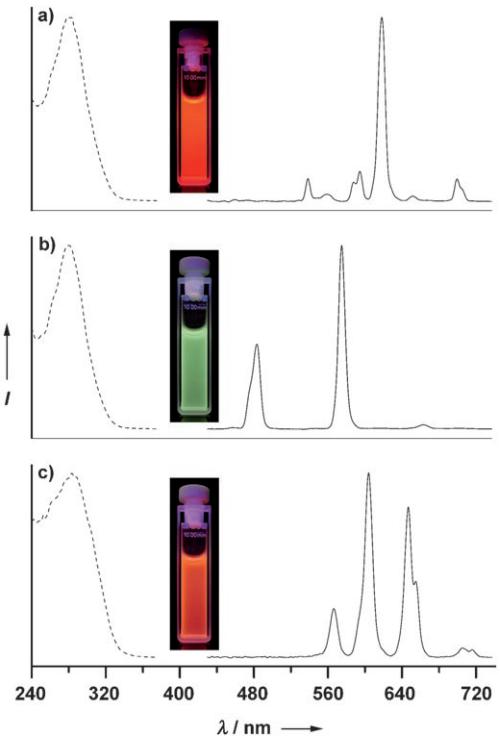

Figure 4. Room-temperature excitation (dashed lines) and emission (solid lines) spectra of a) YVO_4:Eu (5 mol%), b) YVO_4:Dy (5 mol%), c) YVO_4:Sm (5 mol%) nanoparticles in aqueous solutions (1 mM). Insets show photographs demonstrating luminescence from the corresponding nanoparticle solutions.

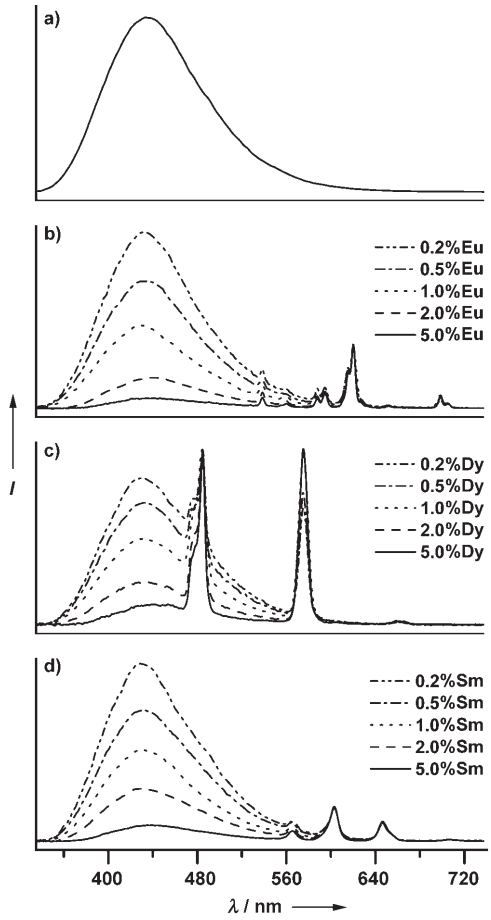

Figure 5. Room-temperature emission spectra of a) $Y(P_{0.75}V_{0.25})O_4$, b) $Y(P_{0.75}V_{0.25})O_4$:Eu (normalized to Eu^{3+} 618 nm emission), c) $Y(P_{0.75}V_{0.25})O_4$:Dy (normalized to Dy^{3+} 485 nm emission), and d) $Y(P_{0.75}V_{0.25})O_4$:Sm (normalized to Sm^{3+} 604 nm emission) nanoparticles upon addition of various concentrations (0.2–5 mol%) of dopants in aqueous solutions (1 mM) under 280-nm excitation.

the activator should be expected (Scheme 1b). Indeed, the P-doped YVO_4 nanoparticles exhibit a broad emission centered at approximately 435 nm (Figure 5a) with a deep blue color upon excitation at 254 nm with a UV lamp (Figure 6a). By subsequently varying the concentration of the Ln dopant, the relative emission intensity of $[VO_4]^{3-}$ to Ln ions can be manipulated with high precision. As shown in Figure 5b–d, $Y(P_{0.75}V_{0.25})O_4$ nanoparticles doped with increasing concentrations of Eu^{3+}, Dy^{3+}, and Sm^{3+} ions (0.2–5 mol%) exhibit decreasing emission intensity ratios of $[VO_4]^{3-}$ to the Ln dopants. As the ion concentration reaches 5 mol%, energy transfer from the $[VO_4]^{3-}$ groups to the Ln dopants becomes efficient; that is, the emission is essentially generated from the latter. This approach allows for selective fine-tuning of the emission color from deep blue to green (Figure 6b–f), red (Figure 6g–k), and yellow (Figure 6l–p). Importantly, the approach can be readily applied to a variety of host–activator systems to expand the emitted color spectrum. Moreover, solid (Ln, P)-doped YVO_4 nanoparticles exhibit the same emission colors as in solutions (Figure 6, top panel), providing evidence for their high stability toward bleaching.

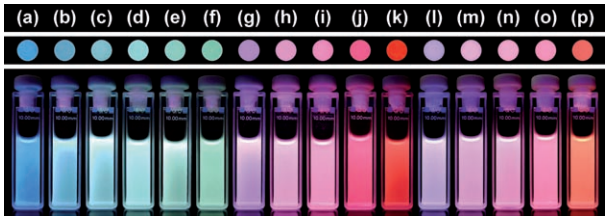

Figure 6. Photographs showing luminescence from (Ln, P)-doped YVO_4 nanoparticles as solids on glass slides (top) and in aqueous solutions (1 mM, bottom). a) $Y(P_{0.75}V_{0.25})O_4$, b–f) $Y(P_{0.75}V_{0.25})O_4$:Dy (0.2, 0.5, 1, 2, and 5 mol%, respectively), g–k) $Y(P_{0.75}V_{0.25})O_4$:Eu (0.2, 0.5, 1, 2, and 5 mol%), l–p) $Y(P_{0.75}V_{0.25})O_4$:Sm (0.2, 0.5, 1, 2, and 5 mol%).

In conclusion, we have presented two complementary approaches to tuning emission colors based upon a single source of YVO_4 nanoparticles doped with Ln and P ions. By precise control of emission wavelengths and intensity ratios through choice of the host–activator systems and control of dopant concentration, the color of emitted light can be easily tuned under single-wavelength excitation. Given the enormous number of available host–activator combinations, the lanthanide-doped nanoparticles should generate a large library of emission spectra in the visible and near-infrared[6h] range with distinguishable spectroscopic fingerprints. Once coupled to biological molecules and refined, the approach should provide a rapid and reliable route to multiplex detection of target biological molecules or materials.

Experimental Section

Reagents: Polyvinylpyrrolidone (PVP, 55 kDa), Na_3VO_4 (99.98%), $Na_2HPO_4{\cdot}12H_2O$ (>99%), NaOH (>98%), $YCl_3{\cdot}6H_2O$ (99.99%), $EuCl_3{\cdot}6H_2O$ (99.99%), $DyCl_3{\cdot}6H_2O$ (99.9%), and $SmCl_3{\cdot}6H_2O$ (99.99%) were purchased from Sigma–Aldrich and used as starting materials without further purification. PVP stock solution (5%) was prepared by dissolving PVP in deionized (DI) water. Na_3VO_4 stock solution (0.095 M) was prepared by dissolving Na_3VO_4 in DI water. Na_3PO_4 stock solution (0.095 M) was prepared by dissolving equimolar amounts of Na_2HPO_4 and NaOH in DI water. $LnCl_3$ (Ln = Y, Eu, Dy, and Sm) stock solutions (0.1 M) were prepared by dissolving the corresponding lanthanide chlorides in DI water.

Nanoparticle synthesis: Na_3VO_4 (1.5 mL) and Na_3PO_4 (4.5 mL) stock solutions were added dropwise to a well-stirred solution of $LnCl_3$ (6 mL) and PVP (3 mL stock solution) at 60 °C. The resulting mixture was stirred for another 10 min, then transferred to a 20-mL teflon-lined autoclave and subsequently heated at 180 °C for 2 h. The obtained nanoparticles were collected by centrifugation, washed with ethanol and DI water several times, and dried in an oven at 50 °C for 24 h.

Characterization: TEM measurements were carried out on a JEOL 2010 transmission electron microscope operating at an acceleration voltage of 200 kV. XRD analysis was carried out on a Siemens D5005 X-ray diffractometer with $Cu_{K\alpha}$ radiation ($\lambda = 1.5406$ Å). The excitation and emission spectra were obtained with a Perkin–Elmer LS55 luminescence spectrometer at room temperature.

Received: October 1, 2007
Published online: December 4, 2007

Keywords: energy transfer · lanthanides · multicolor tuning · nanoparticles

[1] a) W. C. W. Chan, S. Nie, *Science* **1998**, *281*, 2016; b) A. Miyawaki, *Dev. Cell* **2003**, *4*, 295.

[2] a) E. Schröck, S. duManoir, T. Veldman, B. Schoell, J. Wienberg, M. A. Ferguson Smith, Y. Ning, D. H. Ledbetter, I. Bar-Am, D. Soenksen, Y. Garini, T. Ried, *Science* **1996**, *273*, 494; b) J. A. Ferguson, F. J. Steemers, D. R. Walt, *Anal. Chem.* **2000**, *72*, 5618; c) S. R. Nicewarner-Pena, R. G. Freeman, B. D. Reiss, L. He, D. J. Pena, I. D. Walton, R. Cromer, C. D. Keating, M. J. Natan, *Science* **2001**, *294*, 137; d) Y. C. Cao, R. Jin, C. A. Mirkin, *Science* **2002**, *297*, 1536; e) M. Kuang, D. Y. Wang, H. B. Bao, M. Y. Gao, H. Mohwald, M. Jang, *Adv. Mater.* **2005**, *17*, 267; f) L. Wang, C. Y. Yang, W. H. Tan, *Nano Lett.* **2005**, *5*, 37; g) L. Wang, W. H. Tan, *Nano Lett.* **2006**, *6*, 84; h) D. C. Pregibon, M. Toner, P. S. Doyle, *Science* **2007**, *315*, 1393; i) J. Liu, J. H. Lee, Y. Lu, *Anal. Chem.* **2007**, *79*, 4120.

[3] a) T. Ha, T. Enderle, D. S. Chemla, P. R. Selvin, S. Weiss, *Chem. Phys. Lett.* **1997**, *271*, 1; b) F. Kohn, J. Hofkens, R. Gronheid, M. Van der Auweraer, *J. Phys. Chem. A* **2002**, *106*, 4808.

[4] a) L. E. Brus, *Appl. Phys. A* **1991**, *53*, 465; b) C. B. Murray, D. J. Norris, M. G. Bawendi, *J. Am. Chem. Soc.* **1993**, *115*, 8706; c) A. P. Alivisatos, *J. Phys. Chem.* **1996**, *100*, 13226; d) M. A. Hines, P. Guyot-Sionnest, *J. Phys. Chem. B* **1998**, *102*, 3655; e) M. Bruchez, Jr., M. Moronne, P. Gin, S. Weiss, A. P. Alivisatos, *Science* **1998**, *281*, 2013; f) I. L. Medintz, H. T. Uyeda, E. R. Goldman, H. Mattoussi, *Nat. Mater.* **2005**, *4*, 435; g) X. Zhong, Y. Feng, W. Knoll, M. Y. Han, *J. Am. Chem. Soc.* **2003**, *125*, 13559; h) J. Zhao, J. A. Bardecker, A. M. Munro, M. S. Liu, Y. Niu, I.-K. Ding, J. Luo, B. Chen, A. K. Y. Jen, D. S. Ginger, *Nano Lett.* **2006**, *6*, 463.

[5] a) Z. A. Peng, X. G. Peng, *J. Am. Chem. Soc.* **2001**, *123*, 183; b) Y. C. Cao, J. Wang, *J. Am. Chem. Soc.* **2004**, *126*, 14336; c) A. M. Derfus, W. C. W. Chan, S. N. Bhatia, *Nano Lett.* **2004**, *4*, 11; d) M. Sugisaki, H.-W. Ren, K. Nishi, Y. Masumoto, *Phys. Rev. Lett.* **2001**, *86*, 4883; e) M. Y. Han, X. H. Gao, J. Z. Su, S. M. Nie, *Nat. Biotechnol.* **2001**, *19*, 631; f) N. Pradhan, D. Goorskey, J. Thessing, X. Peng, *J. Am. Chem. Soc.* **2005**, *127*, 17586.

[6] a) K. Riwotzki, H. Meyssamy, A. Kornowski, M. Haase, *J. Phys. Chem. B* **2000**, *104*, 2824; b) P. Schuetz, F. Caruso, *Chem. Mater.* **2002**, *14*, 4509; c) J. W. Stouwdam, F. C. J. M. Van Veggel, *Nano Lett.* **2002**, *2*, 733; d) S. Heer, K. Kömpe, H. U. Güdel, M. Haase, *Adv. Mater.* **2004**, *16*, 2102; e) J. Feng, G. M. Shan, A. Maquieira, M. E. Koivunen, B. Guo, B. D. Hammock, I. M. Kennedy, *Anal. Chem.* **2003**, *75*, 5282; f) E. Beaurepaire, V. Buissette, M. P. Sauviat, D. Giaume, K. Lahlil, A. Mercuri, D. Casanova, A. Huignard, J. L. Martin, T. Gacoin, J. P. Boilot, A. Alexandrou, *Nano Lett.* **2004**, *4*, 2079; g) P. R. Diamente, F. C. J. M. van Veggel, *J. Fluoresc.* **2005**, *15*, 543; h) J. W. Stouwdam, M. Raudsepp, F. C. J. M. van Veggel, *Langmuir* **2005**, *21*, 7003; i) F. Wang, W. B. Tan, Y. Zhang, X. P. Fan, M. Q. Wang, *Nanotechnology* **2006**, *17*, R1; j) F. Wang, X. P. Fan, M. Q. Wang, Y. Zhang, *Nanotechnology* **2007**, *18*, 025701.

[7] W. D. Kingery, H. K. Bowen, D. R. Uhlmann, *Introduction to Ceramics*, Wiley, New York, **1976**.

[8] G. Blasse, *Luminescent Materials*, Springer, Berlin, **1994**.

